Digest Journal of Nanomaterials and Biostructures Vol. 14, No. 2, April - June 2019, p. 427 - 437

# FIRST-PRINCIPLES STUDY OF ELECTRONIC STRUCTURAL, ELASTIC, AND THERMODYNAMIC PROPERTIES OF Sn-Bi ALLOYS

X. M. DU, H. T. QI, W. Z. WU, K. F. ZHEN, G. S. GUO*
*School of Materials Science and Engineering, Shenyang Ligong University, Shenyang 110159, China*

Structural, electronic, elastic and thermodynamic properties of the $Sn_xBi_{(16-x)}$ ($x$=7, 9, 10, 12, 13, 14, 15) solid solution alloys with tetragonal structure were investigated by means of first-principles calculations within the framework of density functional theory. The results of enthalpies of formation and cohesive energy show that the stability of the alloys increases with the decrease of the content Bi. The electronic structure was further investigated to understand the underlying mechanism of the structural stability of the $Sn_xBi_{(16-x)}$ alloys. The single-crystal elastic constants were calculated, showing that the $Sn_xBi_{(16-x)}$ alloys are mechanically stable structure. Then the bulk modulus $B$, Young's modulus $E$, shear modulus $G$ and Poison's ratio $\nu$ were estimated for polycrystalline $Sn_xBi_{(16-x)}$ alloys from the elastic constants. The ductility and plasticity of $Sn_xBi_{(16-x)}$ alloys were improved with decrease of the content of Bi. The elastic anisotropy was also further discussed in details. The substitution of Sn atoms by Bi makes the $Sn_xBi_{(16-x)}$ alloys elastically more isotropic for the {001} shear plane along the <010>direction. Finally, thermodynamic properties such as the Debye temperatures, the specific heat, and melting temperature for the $Sn_xBi_{(16-x)}$ alloys were estimated from elastic properties.

(Received December 1, 2018; Accepted May 27, 2019)

*Keywords*: $Sn_xBi_{(16-x)}$ alloys, First-principles calculations, Elastic properties, Thermodynamic properties

## 1. Introduction

Pb-containing solder alloys were widely used in the electronic packaging industry. These alloys are reliable, well tested and quite inexpensive. However, since lead is harmful to human health due to pollution of groundwater, an urgent necessity exists to develop appropriate substitutes for the free lead-free solder alloys. A large variety of lead-free solders have already been developed, mainly involving the Sn-Cu, Sn-Ni and Sn-Ag systems [1]. These new lead-free solders have been identified as the most promising alternatives to the eutectic Sn-Pb solder. However, these new lead-free solders have higher melting point (212℃) than eutectic lead-tin solder (183℃), which is the main issue in the electronic packaging, and too high a soldering temperature coulddamage electronic devices and polymer based printed circuit boards [2, 3].

Sn-Bi solder alloys with low melting temperature (only 138℃ for Sn-58Bi solder alloys) are appropriate for temperature-sensitive components. Many studies, related to microstructure, interfacial intermetallic compounds, mechanical properties, and electromigration property, about Sn-58Bi have been conducted. Felton et al. [4] studied the wetting properties and the effects of aging on the microstructure of Sn-Bi solders. The results show that Sn-Bi solders do not wet bare copper well, but that they do wet copper having a hot-dipped Sn-Bi coating. During aging, tin is depleted from the solder/base metal interface. The two-phase Sn-Bi microstructure coarsens during aging; the rate of coarsening can beslowed by adding 1.0 wt. % Cu to the solder. Huang et al. [5] investigated the interfacial reaction between Sn-57Bi-(Co) and Cu. The results showed that only $Cu_6Sn_5$ phase was formed in molten Sn-57Bi/solid Cu couples, while both $Cu_6Sn_5$ and $Cu_3Sn$

* Corresponding author: 1013508301@qq.com.

phases were formed in solid Sn-57Bi/solid Cu couples. Addition of Co suppressed the formation of $Cu_3Sn$.Yang et al.[6] reported that the microstructure of Sn-Bi composite solder can be refined by increasing alloying with graphite. Zhang and Chen suggested that addition of multi-walled carbon nanotubes could refine thegrains and reduce the Bi content in the deposited Sn-Bi alloy [7]. Song et al.[8] revealed that the Bi-rich precipitates appearing in high-Bi samples lead to quick crack propagation. Adding exotic elements to refine the grain size is viewed asan advisable method to enhance the mechanical properties of Sn-Bi solder. Shen et al. [9] revealed that Cu additions into Sn-Bi alloy refined the grain size of the Bi-rich phase and decreased the interface brittleness and improved the shear strength of Sn-Bi solder joints. In contrast, Zn weakened the shear strength due to the brittle nature of the Zn-rich phase. Li et al. [10] reported that the tensile strength of the Sn-Bi-In solder alloys and solder joints declined with increasing Bi content.

While industrial interest in these solders is increasing, there has been relatively little fundamental research on theirthe structural stability, electronic properties, elastic properties.The present work focuses solely on the DFT based ab initio atomistic computational method to study electronic properties and the elastic properties of Sn-Bi alloys. The study of electronic properties of Sn-Bi alloys is important because the elastic properties are manifestations of the bonding between different elements at the atomic level. Also there is no experimental data available regarding the electronic band structure to study its electronic properties. Further the Debye temperature along with longitudinal, transverseand average sound velocities are calculated at zero pressure.

## 2. Computational methods

The 2×1×1 supercells of $Sn_xBi_{(16-x)}$ ($x$=7, 9, 10, 12, 13, 14, 15) solid solution alloys investigated in this study were constructed mainly based on the Sn-type structural models. The Sn has a Tl2 crystal structure with space group I4/mmm (No.139) where the Sn atom is in 2a (0, 0, 0) Wyckoff site. The tetragonal 2×1×1 supercell contains 16 atoms. The different lattice positions of 2a Wyckoff site in Sn supercell of 2×1×1 are replaced by Bi atom.The series of $Sn_xBi_{(16-x)}$ such as $Sn_7Bi_9$, $Sn_9Bi_7$, $Sn_{10}Bi_6$, $Sn_{12}Bi_4$, $Sn_{13}Bi_3$, $Sn_{14}Bi_2$, $Sn_{15}Bi$, were obtained, where the weight percentages of Bi were 69.3%, 57.7%, 51.3%, 37%, 28.9%, 20.1% and 10.5% respectively. Fig. 1 show the structural models of $Sn_xBi_{(16-x)}$ alloys. According to the Sn-Bi phase diagram, $Sn_7Bi_9$ and $Sn_9Bi_7$ are hypereutectic alloys and the rest is hypoeutectic alloys.

All calculations were performed using Density Functional Theory (DFT) as implemented in the Quantum-ESPRESSO [11]. The ion–electron interaction was modeled by ultrasoft pseudopotentials [12]. Generalized gradient approximation (GGA) with the PBE exchange-correlation functional [13]was used. The kinetic energy cut-off value for plane-wave expansions was set as 380 eV for all the calculations.The larger values of the cut-off energy of atomic wave functions have been tested, such as 400 eV, 450 eV and 500 eV etc. Tests indicated that the total energies of the crystals have been not obviously decreased. The *k*-point meshes for Brillouin zone sampling were constructed using Monkhorst–Pack scheme[14] with 6×3×3 grids for all structural models. Convergence with respect to the *k*-point sampling for the Brillouin zone integration was tested independently on the these alloys using regular meshes of increasing density.Tests indicate that the total energy converges to 1 meV/atom. The valence electronic configurations were taken to be $5s^25p^2$ for Sn, $6s^26p^3$ for Bi. For all structures the lattice parameters, the volume and the atom positions were allowed to relax simultaneously. The relaxations of cell geometry and atomic positions were carried out using a conjugate gradient algorithm until the Hellman–Feynman force on each of the unconstrained atoms was less than 0.01eV/Å. The self-consistent calculations were considered to be converged when the difference in the total energy of the crystal did not exceed $10^{-6}$ eV at consecutive steps. After the structures are optimized, the total energies are recalculated self-consistently with the tetrahedron method [15].The latter technique was also used to calculate the electronic density of states (DOS).

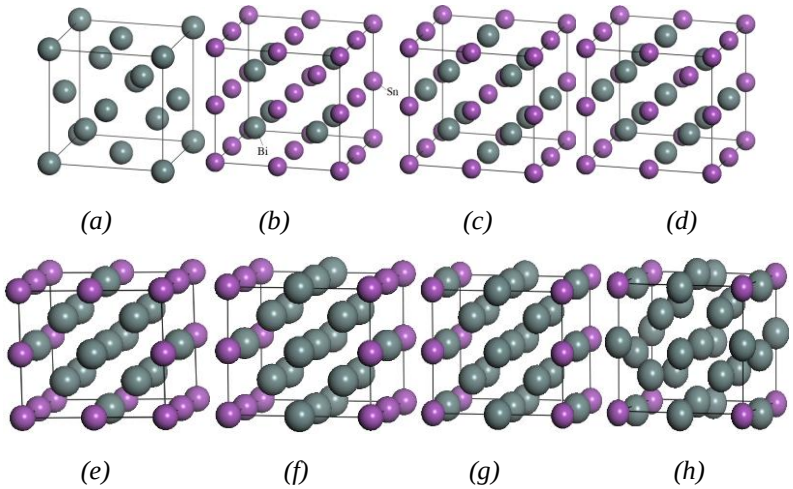


*(a)* *(b)* *(c)* *(d)*

*(e)* *(f)* *(g)* *(h)*

*Fig. 1.Crystal structures of Sn and $Sn_xBi_{(16-x)}$ alloys, (a) Sn, (b) $Sn_7Bi_9$, (c) $Sn_9Bi_7$, (d) $Sn_{10}Bi_6$, (e) $Sn_{12}Bi_4$, (f) $Sn_{13}Bi_3$, (g) $Sn_{14}Bi_2$, (h) $Sn_{15}Bi$.*

## 3. Results and discussion

### 3.1.Phase stability

Generally, the evaluation of the heat of formation per atom isrelative to the composition-averaged energies of the pure elementsin their equilibrium crystal structures [16]. The $H_f$ of $Sn_xBi_{(16-x)}$ structure at a low temperature can be expressed as follows:

$$H_f = (E_{\text{tot}} - N_{\text{Sn}}E_{\text{tot}}(\text{Sn})_{\text{solid}} - N_{\text{Bi}}E_{\text{tot}}(\text{Bi})_{\text{solid}}) / (N_{\text{Sn}} + N_{\text{Bi}}) \quad (1)$$

where $E_{\text{tot}}$ is the total energy of $Sn_xBi_{(16-x)}$ in equilibrium lattice per unit ; $E_{\text{tot}}(\text{Sn})_{\text{solid}}$ and $E_{\text{tot}}(\text{Bi})_{\text{solid}}$ are the total energy of tetragonal Sn and rhombohedral Bi in their stable state per unit cell, respectively; $N_{\text{Sn}}$ and $N_{\text{Bi}}$ refer to the numbers of Sn and Bi atoms in unit cell of $Sn_xBi_{(16-x)}$, repectively. In the present work, we calculate the single atomic energy by the following method: at first, the energy of a pure metal crystal in the solid state was calculated, then the energy was divided by the number of atoms involved in the crystal, and this result is the energy of a single atom in the pure metal. The calculated energies of Sn and Bi pure metals for our considered systems were -87.5691 eV and -147.4482 eV, respectively.The calculated formation enthalpies of $Sn_xBi_{(16-x)}$ alloys are listed in Table 1. Generally, the lower the formation enthalpy is, the more stable the crystal structure is. It was found that the formation enthalpies of $Sn_xBi_{(16-x)}$ alloys decreased with the decrease of the content Bi atoms in structure model, indicating that the stability of the alloys increases correspondingly.

The cohesive energy ($E_{\text{coh}}$) can be expressed as follows:

$$E_{\text{coh}} = (E_{\text{tot}} - N_{\text{Sn}}E_{\text{tot}}(\text{Sn})_{\text{isloated}} - N_{\text{Bi}}E_{\text{tot}}(\text{Bi})_{\text{isloated}}) / (N_{\text{Sn}} + N_{\text{Bi}}) \quad (2)$$

where $E_{\text{tot}}(\text{Sn})_{\text{isloated}}$ and $E_{\text{tot}}(\text{Bi})_{\text{isloated}}$ are the total energy of the isolated constituent atoms at infinite separation.

In order to obtain an accurate value for the cohesive energy, the energy calculations for both isolated atom and the crystal must be performed at the same level of accuracy. The energy of an isolated atom has been calculated using a cubic supercell (irrespective of crystal structure of the corresponding solid) with large lattice parameter of 10Å so that the inter atomic interaction is

negligible. The calculated energies of isolated atoms Sn and Bi are -85.687and -147.4713eV·atom$^{-1}$, respectively. According to Eqs. (2), the obtained cohesive energies of $Sn_xBi_{(16-x)}$ alloys are listed in Table 1. It is found that the cohesive energy of the $Sn_xBi_{(16-x)}$ alloys increases with the decrease of the content Bi atoms in structure model. In general, the cohesive intensity and structural stability of the crystal are correlated with its cohesive energy [17] being defined as eitherthe energy needed to form the crystal from free atoms or the work needed to decompose the crystal into isolated atoms. The larger the cohesive energy, the more stable is the corresponding crystal structure.The resultshave shown that the hypoeutectic Sn-Bi alloys is more stable than hypoeutectic Sn-Bi alloys.

*Table 1.Optimized results for $Sn_xBi_{(16-x)}$ alloys including total energy $E_{tot}$, formation enthalpy $H_f$ and cohesive energy$E_{coh}$.*

| Alloys | $E_{tot}$(eV) | $H_f$(eV) | $E_{coh}$(eV) |
|---|---|---|---|
| $Sn_7Bi_9$ | -1948.1338 | -0.5073 | -1.318 |
| $Sn_9Bi_7$ | -1832.0751 | -0.7385 | -1.787 |
| $Sn_{10}Bi_6$ | -1773.6549 | -0.8297 | -1.997 |
| $Sn_{12}Bi_4$ | -1655.5498 | -0.9330 | -2.339 |
| $Sn_{13}Bi_3$ | -1596.5086 | -0.9854 | -2.510 |
| $Sn_{14}Bi_2$ | -1538.4379 | -1.098 | -2.742 |
| $Sn_{15}Bi$ | -1479.4521 | -1.154 | -2.917 |

### 3.2.Electronic structure

To further understand the formation mechanisms, the electronic properties of $Sn_xBi_{(16-x)}$ alloys were analyzed based on the total and partial densities of states (DOS and PDOS) of these alloys, as shown in Fig. 2. It could be found that the hybridization of Sn-s and Bi-p, Sn-p and Bi-s states was believed to be the dominant factor for the stability improvement of $Sn_xBi_{(16-x)}$ alloys. It can be seen from Fig. 2 that the main bonding peaks of $Sn_xBi_{(16-x)}$ alloys locate in the range from −13 eV to 3 eV, originating from the contribution of valance electron numbers of Sn-5s, Sn-5p, Bi-6s, Bi-6p.The bonding peaks appeared in the energy range from -13 eV to -9.5 eV, which were formed by the hybridization between the Bi-6s orbit and the Sn-5p, Sn-5s orbits. The bonding peaks appeared in the energy range from -9.0 eV to -5.0 eV were formed by the hybridization between the Sn-5s orbit and the Bi-6p, Bi-6s orbits. For the bonding peaks in the energy range from -5.0 eV to 3.0 eV, the hybridization between the Sn-5p orbit and the Bi-6p orbit was predominant. As the content of Bi in $Sn_xBi_{(16-x)}$ alloys decreased, the hight of the bonding peaks between around -13 eV and -9.5 eV decreased. It is indicated that the hybridization between the Bi-6s orbit and the Sn-5p, Sn-5s orbits is continually weakening. Moreover, the values of the total DOS at Fermi level are larger than zero for $Sn_xBi_{(16-x)}$ alloys, which indicats the metallic behavior.The bonding electron numbers at the Fermi level, $N(E_F)$ for $Sn_7Bi_9$, $Sn_9Bi_7$, $Sn_{10}Bi_6$, $Sn_{12}Bi_4$, $Sn_{13}Bi_3$, $Sn_{14}Bi_2$, $Sn_{15}$Biis 9.1, 8.9, 8.7, 8.6, 8.3, 7.6, 7.4, respectively. In general, $N(E_F)$ on DOS plot can be used to characterize the activity of valance electrons of the atoms in crystal. Namely, the smaller $N(E_F)$, the less is change probability of the electronic structures of the crystal when external conditions change, thus the crystal has the higher stability [18]. The stability of $Sn_xBi_{(16-x)}$ alloys improved with the decrease of the content of Bi, which are entirely consistent with the results of the calculated enthalpies of formation cohesive energies.

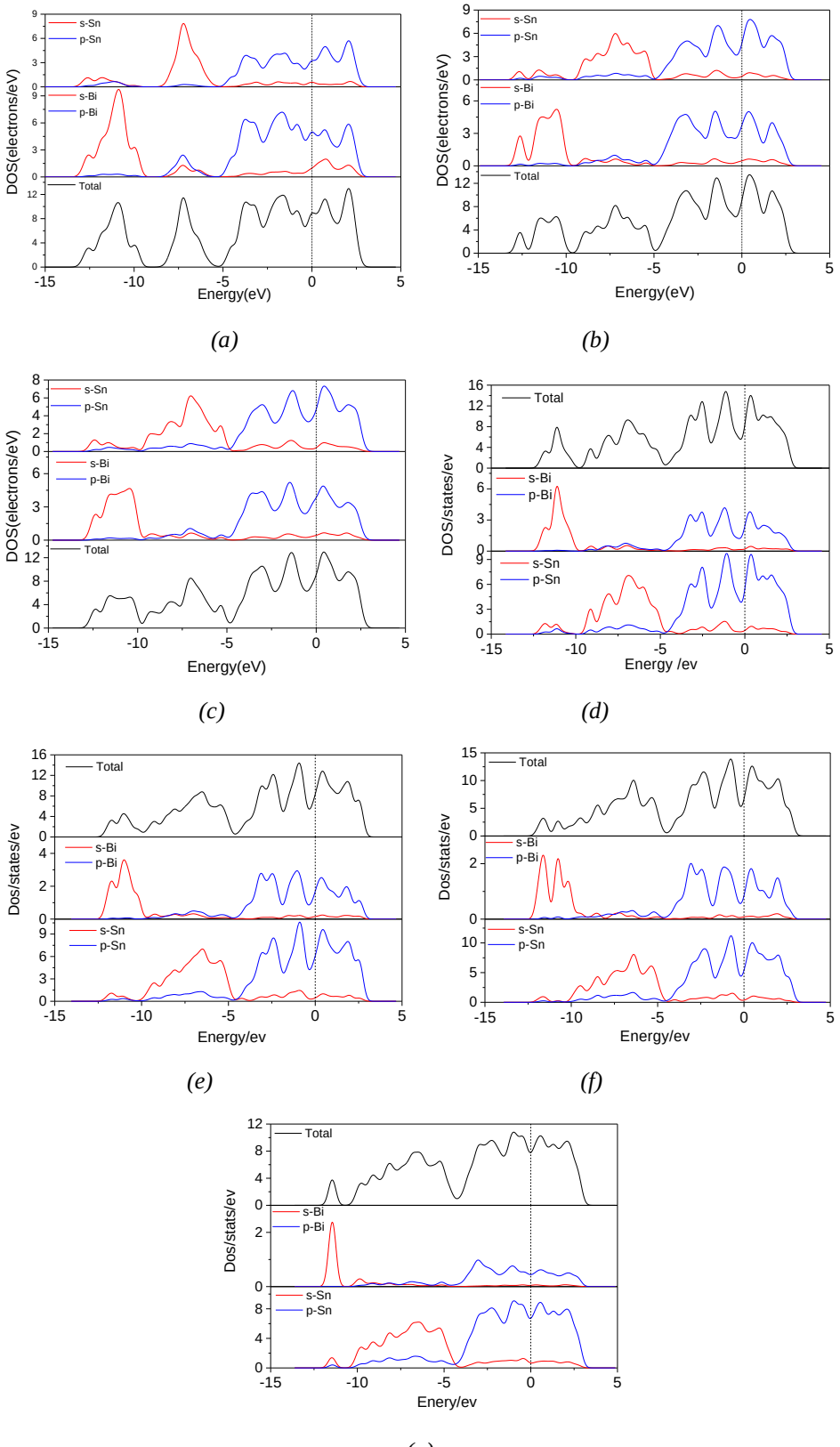


*Fig. 2.The calculated total density of states and partial densities of states of $Sn_xBi_{(16-x)}$ alloys, (a) $Sn_7Bi_9$, (b) $Sn_9Bi_7$, (c) $Sn_{10}Bi_6$, (d)$Sn_{12}Bi_4$, (e) $Sn_{13}Bi_3$, (f) $Sn_{14}Bi_2$, (g) $Sn_{15}Bi$.*

### 3.3. Elastic properties

Elastic constants are the measure of the resistance of a crystal to an externally applied stress. Through imposing small strain on the perfect lattice, the elastic constants can be obtained. For tetragonal $Sn_xBi_{(16-x)}$ crystals, there are six independent elastic constants, i.e., $C_{11}$, $C_{12}$, $C_{13}$, $C_{33}$, $C_{44}$ and $C_{66}$. The calculated elastic constants at the ground states are listed in Table 2.

The elastic stability is an ecessary condition for a solid to exist.The intrinsic mechanical stability of a solid is in general determined by certain conditions related to the crystal symmetry [19] and the following criteria based on relations between elastic constants have to be fulfilled.

For tetragonalphases,

$$C_{11}+C_{33}-2C_{13}>0,\ \ 2C_{11}+C_{33}+2C_{12}+4C_{13}>0 \ \text{ and } \ (2C_{11}+C_{33})/3-B>0 \qquad (3)$$

As shown in Table 2, all the elastic constants of $Sn_xBi_{(16-x)}$ alloys satisfy the above restrictions, so all these structures are mechanically stable.

*Table 2.The calculated elastic constants, $C_{ij}$ (in GPa) for $Sn_xBi_{(16-x)}$ (x=7, 9, 10, 12, 13, 14, 15) alloys.*

| Alloys | $C_{11}$ | $C_{12}$ | $C_{13}$ | $C_{33}$ | $C_{44}$ | $C_{66}$ |
|---|---|---|---|---|---|---|
| $Sn_7Bi_9$ | 60 | 36.9 | 88.1 | 220.2 | 44.8 | 44.7 |
| $Sn_9Bi_7$ | 58.3 | 37.4 | 89.2 | 222.6 | 42.4 | 43.6 |
| $Sn_{10}Bi_6$ | 56.4 | 38.1 | 90.8 | 224.5 | 38.1 | 41.4 |
| $Sn_{12}Bi_4$ | 54.7 | 39.2 | 91.9 | 225.3 | 36.3 | 38.3 |
| $Sn_{13}Bi_3$ | 53.4 | 40.5 | 93.1 | 226.2 | 34.9 | 35.9 |
| $Sn_{14}Bi_2$ | 52.7 | 41.9 | 94.6 | 227.6 | 32.6 | 33.8 |
| $Sn_{15}Bi$ | 51.1 | 43.1 | 96.4 | 229.3 | 30.2 | 30.6 |

The elastic properties of polycrystalline materials are usually characterized by the elastic moduli, suchas bulk modulus($B$), Young's modulus($E$), shear modulus($G$) and Poisson ratio $\nu$. The bulk $B$ and the shear modulus $G$ for tetragonal crystal structure are taken as [20]:

$$B=2/9(C_{11}+C_{12}+2C_{13}+C_{33}/2) \qquad (4)$$

and

$$G=1/15(2C_{11}+C_{33}-C_{12}-2C_{13}+6C_{44}+3C_{66}) \qquad (5)$$

Then, Young's modulus $E$ and Possion's ratio $\nu$ can be calculated by [21]:

$$E\ =9BG/(3B+G) \qquad 6)$$

and

$$\nu=(3B-2G)/(6B+2G) \qquad 7)$$

All calculated results based on Eqs. (4)-(7) are listed in Table 3. It can be found that the

calculated bulk modulus $B$ increase and Young's modulus $E$, shear modulus $G$ decrease with decrease of the content of Bi in $Sn_xBi_{(16-x)}$ alloys. It is indicated that the capability of plastic deformation of $Sn_xBi_{(16-x)}$ alloys increases with decrease of the content of Bi. On the other hand, Poisson's ratio $\nu$ is used to quantify the stability of the crystal against shear, which can provide more information on the characterizations of the bonding forces than elastic constants [22]. The larger the Poisson's ratio is, the better the plasticity is. In this work, the calculated values of $\nu$ increase with decrease of the content of Bi in $Sn_xBi_{(16-x)}$ alloys, as listed in Table 3, which indicates that the plasticity of $Sn_xBi_{(16-x)}$ alloys are improves.

The ratio of the bulk modulus to shear modulus of crystalline phases, proposed by Pugh [23], can empirically predict the brittle and ductile behavior of materials. A high $B/G$ ratio is associated with ductility, whereas a low value corresponds to brittle nature. The critical value which separates ductile and brittle material is around 1.75. The calculated results in Table 3 show that $Sn_xBi_{(16-x)}$ alloys exhibit good ductility. Besides $B/G$, the ductility behavior was also proposed to be related to the so-called Cauchy pressures[24]. For phases with tetragonal symmetry, the Cauchy pressures aredefined as:

$$C1 = C_{12} - C_{66} \tag{8}$$

$$C2 = C_{13} - C_{44} \tag{9}$$

Positive or negative values of $C1$ and $C2$ indicate ductile or brittle behavior, respectively. The calculated values of $C1$ and $C2$ were shown in Table 3. It can be seen that despite the fact that the Cauchy pressures $C1$ for $Sn_7Bi_9$, $Sn_9Bi_7$, $Sn_{10}Bi_6$ are negative, to a certain extent, that should indicate the brittle behavior, both $C1$ and $C2$ of all $Sn_xBi_{(16-x)}$ alloys exhibit general trend to have higher values as the Bi content decreases. This indicates that the ductility of $Sn_xBi_{(16-x)}$ alloys are improved with decrease of the content of Bi.

The elastic anisotropy of crystal is closely correlated with the possibility to induce microcracks and dislocations in the materials [25,26]. The shear resistance of crystal (the energy change in a crystal associated with the shear modes along different slip directions) is characterized by the elastic anisotropy factors. In the tetragonal crystal, the anisotropic behavior can be described by elastic anisotropy factors:

$$A_1 = 2C_{66} / (C_{11} - C_{12}) \tag{10}$$

$$A_2 = 4C_{44} / (C_{11} + C_{33} - 2C_{13}) \tag{11}$$

$$A_3 = C_{44} / C_{66} \tag{12}$$

$A_1$, $A_2$ and $A_3$is corresponding to the {001} shear plane along the <010>direction, the {011} shear plane along the <011>direction and {100}shear plane along the <100>direction,respectively. For anisotropic crystal the factors $A_1$, $A_2$ and $A_3$ must be unity. The deviation of the anisotropic factors from unity is a measure for the elastic anisotropy. The calculated values of the elastic anisotropy factors for $Sn_xBi_{(16-x)}$ alloys listed in Table 3. The evident correlation between the values of elastic anisotropy factors and number of Bi atoms in $Sn_xBi_{(16-x)}$ was found: the $A_1$ elastic anisotropy factors increases with decreasing number of Bi atoms whereas $A_2$ decreases. This means that the substitution of Sn atoms by Bi makes the $Sn_xBi_{(16-x)}$ alloys elastically more isotropic, especially for the {001} shear plane along the <010>direction.

*Table 3.The calculated bulk modulus B (GPa), shear modulus G (GPa), Young's modulus E (GPa), B/G, Poisson's ratio v, anisotropic index $A_1$, $A_2$and $A_3$ for $Sn_xBi_{(16-x)}$ (x=7, 9, 10, 12, 13, 14, 15) alloys.*

| Alloys | *B* | *G* | *E* | *B/G* | *v* | *C*1 | *C*2 | $A_1$ | $A_2$ | $A_3$ |
|---|---|---|---|---|---|---|---|---|---|---|
| $Sn_7Bi_9$ | 93.4 | 35.3 | 94.1 | 2.64 | 0.33 | -7.8 | 43.3 | 3.87 | 1.72 | 1.00 |
| $Sn_9Bi_7$ | 94.0 | 33.9 | 90.8 | 2.77 | 0.33 | -6.2 | 46.8 | 4.17 | 1.65 | 0.97 |
| $Sn_{10}Bi_6$ | 94.8 | 31.4 | 84.7 | 3.02 | 0.35 | -3.3 | 52.7 | 4.52 | 1.53 | 0.92 |
| $Sn_{12}Bi_4$ | 95.5 | 29.6 | 80.5 | 3.22 | 0.36 | 0.9 | 55.6 | 4.94 | 1.51 | 0.95 |
| $Sn_{13}Bi_3$ | 96.4 | 28.2 | 77.1 | 3.41 | 0.37 | 4.6 | 58.2 | 5.56 | 1.49 | 0.97 |
| $Sn_{14}Bi_2$ | 97.7 | 26.6 | 73.1 | 3.67 | 0.38 | 8.1 | 62 | 6.25 | 1.43 | 0.96 |
| $Sn_{15}Bi$ | 98.8 | 24.6 | 68.1 | 4.02 | 0.39 | 12.5 | 66.2 | 7.65 | 1.38 | 0.99 |

### 3.4. Thermodynamic properties

The Debye temperature $\theta_D$ is a fundamental attribute of a solid connecting elastic properties with thermodynamic properties such as specific heat, sound velocity and melting temperature. It can be calculated from the averaged sound velocity, $v_m$ by the following equation [27]:

$$\theta_D = \frac{h}{k_B}\left[\frac{3n}{4\pi}\left(\frac{N_A\rho}{M}\right)\right]^{\frac{1}{3}} v_m \tag{13}$$

where h is Planck's constant, $k_B$ is Boltzmann's constant, $N_A$ is Avogadro's number, $n$ is the number of atoms in the unit cell, $M$ is the molecular weight and $\rho$ is the density. The average sound velocity in the polycrystalline material is approximately given by [27]:

$$v_m = \left[\frac{1}{3}\left(\frac{2}{v_s^3} + \frac{1}{v_l^3}\right)\right]^{-1/3} \tag{14}$$

where$v_l$ and $v_s$ are the longitudinal and transverse sound velocity, respectively, which can be obtained using the shear modulus $G$ and the bulk modulus $B$ from Navier's equations [28]:

$$v_l = \sqrt{\frac{B + 4G/3}{\rho}} \text{ and } v_s = \sqrt{\frac{G}{\rho}} \tag{15}$$

The calculated values of sound velocity and Debye temperature as well as the density for the $Sn_xBi_{(16-x)}$ alloys are given in Table 4. The Debye temperature of $Sn_xBi_{(16-x)}$ alloys increases with decreasing numberof Bi atoms. As a rule of thumb, a higher Debye temperature means a larger associated thermal conductivity [29]. Therefore,the decrease of Bi content can improve thermal conductivity of $Sn_xBi_{(16-x)}$ alloys.

The melting temperature is considered to be an important index to evaluate heat resistance of alloy materials. For tetragonal structural metals, the melting temperature, $T_m$ can be expressed as[30]:

$$T_m = 254\text{K} + (4.50\text{K/GPa})[1/3(2C_{11} + C_{33})] \pm 300\text{K} \tag{16}$$

In present work, a minus sign can be slected in the Eq. (16). The calculated values of the melting temperature for $Sn_xBi_{(16-x)}$ are listed in Table 4. It can be seen that the melting temperature decreases with the decreasing number of Bi atoms. It can be understood due to higher Young's modulus, shear modulus for those alloys.

In the approximation of Debye model, the specific heat of the solid, $C_v$ can be obtained from Debye temperature by the following equation [31]

$$C_v = 9N_A k_B (T/\theta_D)^3 \int_0^{\theta_D/T} \frac{x^4 e^x}{(e^x-1)^2} dx \quad (17)$$

where $T$ is the temperature (K).

The calculated values of the specific heat of $Sn_xBi_{(16-x)}$ alloys the are shown in Fig. 3. The specific heat of these alloys is similar and increases with increasing temperature below $\theta_D$. However, the specific heat of these alloys is gradually close to 25 J/mol·K for the high temperature case ($T>>\theta_D$), which is the Dulong-Petit result (equal to $3N_Ak_B$) from classical thermodynamics. For low temperature case ( $T<<\theta_D$), the electron specific heat becomes significant for metals and is combined with the above specific heat in the Einstein-Debye specific heat [32].

*Table 4. The calculated density ($\rho$), the longitudinal, transverse, and average sound velocity ($v_l$, $v_s$, $v_m$), the Debye temperatures ($\theta_D$) and the melting temperature ($T_m$).*

| Phase | $v_l$ (m·s$^{-1}$) | $v_s$(m·s$^{-1}$) | $v_m$(m·s$^{-1}$) | $\rho$ (kg·m$^{-3}$) | $\theta_D$ (K) | $T_m$ (K) |
|---|---|---|---|---|---|---|
| $Sn_7Bi_9$ | 3541 | 3125 | 3242 | 9561 | 313 | 464 |
| $Sn_9Bi_7$ | 36171 | 3209 | 33242 | 9125 | 323 | 462 |
| $Sn_{10}Bi_6$ | 36591 | 3276 | 3386 | 8832 | 329 | 459 |
| $Sn_{12}Bi_4$ | 3871 | 3486 | 3597 | 7854 | 345 | 456 |
| $Sn_{13}Bi_3$ | 39391 | 3567 | 3675 | 7576 | 353 | 453 |
| $Sn_{14}Bi_2$ | 4018 | 3662 | 3766 | 7284 | 362 | 453 |
| $Sn_{15}Bi$ | 4077 | 3743 | 3842 | 7054 | 371 | 451 |

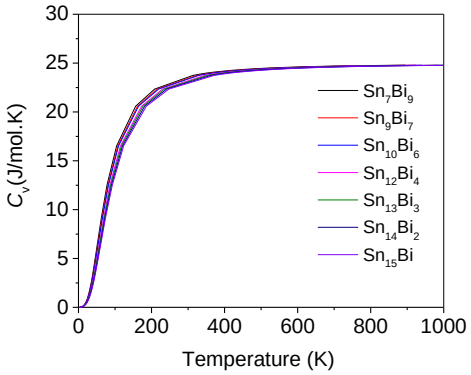


*Fig. 3.The dependence of specific heat on temperature for $Sn_xBi_{(16-x)}$ alloys.*

## 4. Conclusions

In summary, we have calculated and analyzed the structural, electronic, elastic and thermodynamic properties of the $Sn_xBi_{(16-x)}$ alloys by the plane-wave ultrasoft pseudopotential method based on the density-functional theory. The calculated enthalpies of formation and cohesive energy reveal that the stability of $Sn_xBi_{(16-x)}$ alloys increases with the decrease of the content Bi. Electronic densities of states haves hown that the s-p and p-p hybridizationsin $Sn_xBi_{(16-x)}$ alloys becomes continually weakening, as the content of Bi decreased.Then the bulk modulus $B$,

Young's modulus *E*, shear modulus *G* and Poison's ratio $\nu$ were estimated for polycrystalline $Sn_xBi_{(16-x)}$ alloys from the elastic constants. The ductility and plasticity of $Sn_xBi_{(16-x)}$ alloys were improved with decrease of the content of Bi. The elastic anisotropy was also further discussed in details. The substitution of Sn atoms by Bi makes the $Sn_xBi_{(16-x)}$alloys elastically more isotropic for the {001} shear plane along the <010>direction. Finally, thermodynamic properties such as the sound velocity, the Debye temperatures, the specific heat, and melting temperature for the $Sn_xBi_{(16-x)}$ alloys were also derived from elastic properties.

**Acknowledgement**

This work was supported by Shenyang Science and Technology Project (No.18-013-0-33), Shenyang Young and Middle-aged Science and Technology Innovation Talents Project (RC180214) in Liaoning Province, China.

## References

[1] H. J. Jiang, K. S. Moon, F. Hua,Chemistry of Materials**19**, 4482 (2007).
[2] M. N. Islam, Y. C. Chan, A. Sharif, M. J. Rizvi, J. Alloys Compd. **396**, 217 (2005).
[3] C. Andersson, C. D. Zou, B. Yang, ESTC Conference in London in September, 2008, pp. 915-921.
[4] L. E. Felton, C. H. Raeder, D. B. Knorr, JOM **7**, 28 (1993).
[5] Y. Huang, S. Chen, J. Electron. Mater.**40**, 62 (2011).
[6] L. Yang, C. C. Du, J. Dai, J. Mater. Sci. **24**, 4180 (2014).
[7] S. H. Zhang, Q. F. Chen, Compos. B Eng. **58**, 275 (2014).
[8] J. M. Song, T. S. Lui, Y. L. Chang, J. Alloys Compd. **403**,191 (2005).
[9] J. Shen, Y. Pu, H. Yin, Q. Tang, J. Electron. Mater. **44**, 532 (2015).
[10]Q. Li, N. Ma, Y. Lei, J. Lin, H. Fu, J. Gu, J. Electron. Mater. **45**, 5800 (2016).
[11] http://www.quantum-espresso.org/ .
[12] D. R. Hamann, M. Schluter, C. Chiang, Phys. Rev. Lett. **43**, 1494 (1979).
[13] J. P. Perdew, K. Burke, M. Ernzerhof, Phys. Rev. Lett. **77**, 3865 (1996).
[14] H. J. Monksorst, J. D. Pack, Phys. Rev. B **13**, 5188 (1976).
[15] P. E. Blochl, O. Jepsen, O. K. Andersen, Phys. Rev. B **49**, 16223 (1994).
[16] G. Ghosh, M. Asta, J. Mater. Res. **20**, 3102 (2005).
[17] V. I. Zubov, N. P.Tretiakov, J. N.Teixeira Rabelo, J. F.Sanchezortiz, Phys. Lett. A **198**, 470 (1995).
[18] Y. Imai, M. Mukaida, T. Tsunoda, Intermetallics, **8**, 381 (2000).
[19] D. C. Wallace, Thermodynamics of Crystals, Wiley, New York (1972).
[20] M. Alouani, R. C. Albers, Phys. Rev. B **43**, 6500 (1991).
[21] A. M. Hao, X. C. Yang, X. M. Wang, Y. Zhu, X. Liu, R. P. Liu, J. Appl. Phys. **108**, 063531 (2010).
[22] B. Mayer, H. Anton, E. Bott, M. Methfessel, J. Sticht, P. C. Schmidt, Intermetallics **11**, 23 (2003).
[23] S. F. Pugh, Phil. Mag. **45**, 823 (1954).
[24] D. G. Pettifor, Philosophical Transactions of the Royal Society A **334**, 439 (1991).
[25] J. R. Rice, J. Mech, Phys. Solids **40**, 239 (1992).
[26] V. Tvergaard, J. W. Hutchinson, J. Am. Ceram.Soc. **71**, 157 (1988).
[27] O. L. Anderson, J. Phys. Chem. Solids, **24**, 909 (1963).
[28] E. Schreiber, O. L. Anderson, N. Soga, Elastic constants and their measurements, New York, McGraw-Hill, 1973.
[29] W. C. Hu, Y. Liu, D. J. Li, X. Q. Zneg, C. S. Xu, Comput. Mater. Sci. **83**, 27(2014).

[30] M. E. Fine, L. D. Brown, H. L. Marcus, Scr. Metall. **18**, 951 (1984).
[31] M. A. Blanco, E. Francisco, V. Luana, Comput. Phys. Commun. **158**, 57 (2004).
[32] http://hyperphysics.phy-astr.gsu.edu/Hbase/Solids/phonon.html.